

## Surrogate modelling for high-lift multi-element hydrofoil shape optimization of a hydrokinetic turbine blade

Rubio-Clemente A<sup>1,2</sup>., Aguilar J<sup>2</sup>., Chica E<sup>2</sup>

<sup>1</sup> Facultad de Ingeniería, Tecnológico de Antioquia–Institución Universitaria TdeA, Calle 78b, No. 72A-220, Medellín, Colombia.

<sup>2</sup> Departamento de Ingeniería Mecánica, Facultad de Ingeniería, Universidad de Antioquia UdeA, Calle 70, No. 52-21, Medellín, Colombia.

Phone/Fax number: +0057 2195547, e-mail: ainhoarubioclem@gmail.com

### Abstract

The hydrodynamic shape of a blade is one of the most important factors in the design process of a horizontal axis hydrokinetic turbine that influences its performance. The present work is focused on the design and hydrodynamic analysis of a high-lift system using the optimization method of surrogate models and computational fluid dynamics (CFD) analysis.

The parameters that affect the amount of the lift and the drag force that a hydrofoil can generate are the gap, the overlap, the flap deflection angle ( $\delta$ ), the flap chord length ( $C_2$ ) and the angle of attack of the hydrofoil ( $\alpha$ ). These factors were varied to examine the turbine performance in terms of the ratio between the lift ( $C_L$ ) and the drag coefficient ( $C_D$ ), and the minimum negative pressure coefficient ( $\min C_{pre}$ ) in order to avoid the cavitation inception. For this propose, surrogate models were implemented to analyse the CFD results and find the optimal combination of the design parameters of the high-lift hydrofoil. The traditional Eppler 420 hydrofoil was utilized for the design of the multi-element profile, which was composed of a main element and a flap. The multi-element design selected as optimal had a gap of 2.825 % $C_1$ , an overlap of 8.52 % $C_1$ , a  $\delta$  of 19.765°, a  $C_2$  of 42.471 % $C_1$  and a  $\alpha$  of -4°, where  $C_1$  refers to the chord length of the main element. In comparison with the traditional Eppler 420 hydrofoil,  $C_L/C_D$  ratio increases from 39.050 to 42.517.

**Key words.** Horizontal axis hydrokinetic turbine, surrogate model, computational fluid dynamics, high-lift system, multi-element hydrofoil

### 1. Introduction

A main objective of hydrokinetic turbine designers is to maximize the performance and reduce manufacture costs [1-2]. One possible way to reach the objective of maximizing the power coefficient ( $C_p$ ) is to design high-lift systems consisting of a hydrofoil with a flap [3-4]. This geometrical configuration results in the maximization of the lift and the minimization of the flow separation around the hydrofoil [4]. Commonly, flow separation leads to a loss of the lift, an increase of the drag and, therefore, a reduction of the blade performance [3-5].

High-lift systems typically require a lot of time to be designed and tested. However, the most recent advances in computational fluid dynamics (CFD) have become in an invaluable tool for hydrodynamic optimization design [6]. In the process of the design optimization, the number of the objective function evaluations using high-fidelity CFD analysis solvers is severely limited by time and cost [8]. One alternative is to construct a simple approximate model of the complicated CFD analysis solver [8]. The approximate model expresses the relationship between the objective function (output) and the design variables (input) with a simple equation. It is important to note that this model requires very little time to evaluate the objective(s) function(s) [8] compared to CFD analysis. In consequence, it allows saving a lot of computational time and exploring a wider design space. Additionally, surrogate models (SM) are used for representing non-linearity of hydrodynamic problems [9]. Therefore, SM, also so-called low fidelity models, are becoming popular [10-11].

SM are successfully used by various researches to optimize wind turbine performance [11-12]. These authors reported that SM are very efficient in comparison with the conventional optimization methods [11-12]. However, the optimization of multi-element hydrofoils for hydrokinetic turbines using SM has not been employed in the literature. In this study, the application of SM is extended to optimize the performance of a multi-element hydrofoil for a horizontal axis hydrokinetic turbine. The details of the mathematical model utilized, meshing schemes employed and the computational analyses conducted are described.

This research uses Ansys Fluent software, as the high fidelity hydrodynamic characteristic evaluator of multi-element hydrofoil. In the software, the objective functions, consisting of the maximization of the lift coefficient ( $C_L$ ) and the minimization of the drag coefficient ( $C_D$ ) of the hydrofoil are evaluated for several initial design parameter combination. From the CFD results and using an iterative procedure, several SM, based on Kriging method, were generated. In each stage and using a genetic algorithm optimizer, new design

points are suggested from the previous created models until the optimal design parameter configuration is found.

## 2. Optimization methodology

In general, the objective of the hydrodynamic shape optimization, for a given operating condition, is to design a hydrofoil that maximizes  $C_L$ , or minimizes  $C_D$ , or maximizes the lift-to-drag ratio ( $C_L/C_D$ ); which is subjected to several constraints, such as the minimum negative pressure coefficient ( $\min C_{pre}$ ) for avoiding the cavitation inception, as well as geometrical constraints, among others [1, 3-5, 13-14].

### 2.1 Cavitation criteria

Cavitation is an undesirable phenomenon that should be considered on the hydrokinetic turbine design. It causes noise, vibration, damage to the turbine components in special the blades, reduces its performance and life. It phenomenon is usually originated in the blade section where the pressure decreases below the vapour pressure of the fluid. The liquid vaporizes instantly, forming a cavity of vapour, which alters the flow [14-15].

The size and shape of the cavity of vapour or vapour bubble also vary due to the pressure and velocity fields. When the vapour cavity collapse suddenly, the pressure on the blade surface increases, promoting erosion on the surface of blade [13-15].

The failures generated by the cavitation decrease the lift and increase the drag [13-15], leading to a reduction of the turbine efficiency. It can be predicted by comparing the local pressure distribution or the local minimum pressure coefficient ( $C_{pre}$ ) with the cavitation number ( $\sigma$ ), which is defined in Eq. (1).

$$\sigma = \frac{P_0 - P_V}{0.5\rho V_{rel}^2} = \frac{P_{AT} + \rho gh - P_V}{0.5\rho V_{rel}^2} \quad (1)$$

where  $P_0$ , is the reference static pressure,  $P_{AT}$  refers to the atmospheric pressure,  $\rho$  is the water density,  $g$  is the

gravity,  $h$  is the distance between the water free surface and the centre on the hydrokinetic rotor,  $P_V$  refers to the vapour pressure at the flow temperature, and  $V_{rel}$  is the relative velocity on a blade section. The  $\min C_{pre}$  is an important parameter at the hydrokinetic turbine design. It gives information on the hydrodynamic loading of the blade and is defined as the minimum value of the pressure coefficient on the suction side of the blade section [14-15].

There will be cavitation on the blade section if the local minimum pressure coefficient,  $\min C_{pre}$  is lower than  $\sigma$ ; therefore, the criterion to avoid cavitation is given by Eq. (2) [14].

$$\sigma + \min C_{pre} \geq 0 \quad (2)$$

The pressure coefficient is classically defined as represented by Eq. (3).

$$C_{pre} = \frac{P_L - P_0}{0.5\rho V_{rel}^2} \quad (3)$$

where  $P_L$  is the local pressure.

### 2.2 Objective functions

In this study, the objective functions were related to the maximization of the  $C_L$  and the minimization of  $C_D$  of the multi-element hydrofoil, as illustrated in Figure 1. Particularly, the optimization problem was formulated as defined in Eq. (4), which was subjected to the restriction described in Eq. (5).

$$\begin{aligned} \max C_L \text{ or } -\min C_D \\ \min C_D \end{aligned} \quad (4)$$

$$|\min C_{pre}| \leq 4 \quad (5)$$

where  $\min C_{pre}$  refers to the minimum negative pressure coefficient to avoid the cavitation inception.

The design parameters are listed in Table 1.

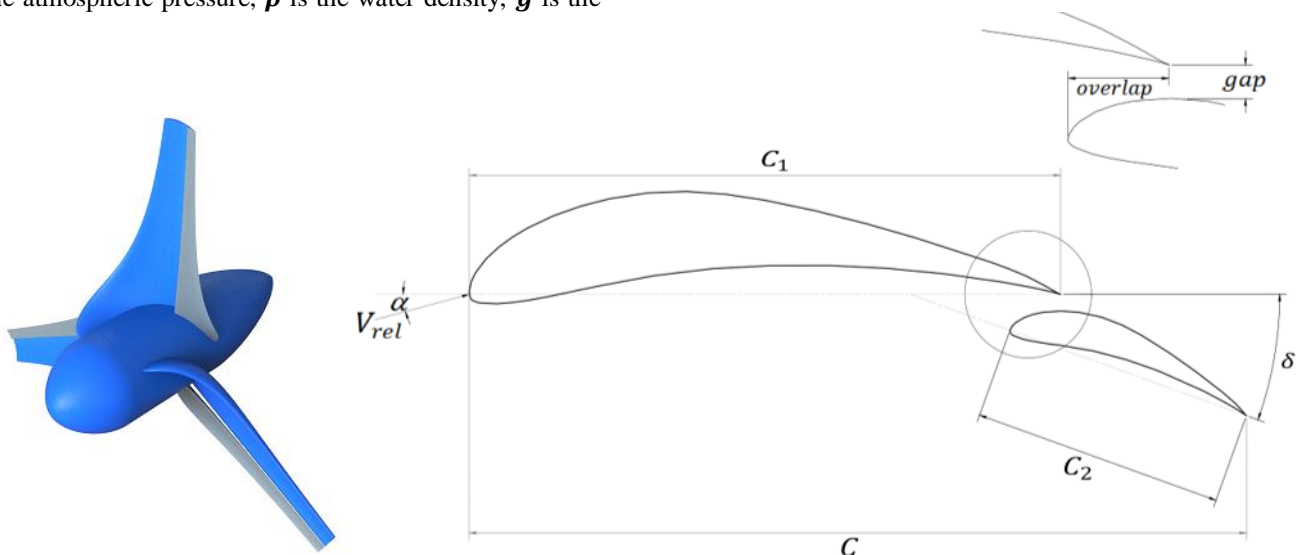


Fig. 1. Geometry parametrization of the multi-element hydrofoil.

Table 1. Multi-element hydrofoil parameter design values.

Parameter (units)	Values
C (m)	0.1773
$V_{rel} = U_{\infty}$ (m/s)	5.517
$\alpha$ (°)	$-10^{\circ} \leq \alpha \leq 10^{\circ}$
$\delta$ (°)	$10^{\circ} \leq \delta \leq 30$
gap (°)	$1\%C_1 \leq gap \leq 5\%C_1$
ovl (m)	$-5\%C_1 \leq ovl \leq 20\%C_1$
$C_2$ (m)	$30\%C_1 \leq C_2 \leq 75\%C_1$

where  $C_L$ ,  $C_D$ , and  $\alpha$  correspond to the lift coefficient, the drag coefficient, and the angle of attack, respectively. The position (gap, overlap) and inclination ( $\delta$ ) of the flap respect to main hydrofoil are the design parameters. Overlap (ovl) is the flap leading-edge position on the x-axis and gap is the flap leading-edge position on the y-axis. In turn, C, which is equal to 0.1773 m in this study,  $C_1$  and  $C_2$ , are the chord length of the blade, the length of the main element and length of flap, respectively [3-5]. It is noteworthy that changing the values of the gap and the overlap slightly resulted in a significantly different hydrodynamic performance for the multi-element hydrofoil.

The design variable vector can be written as described by Eq. (6).

$$X = [\alpha, \delta, gap, ovl, C_2]^T \quad (6)$$

The size of the chord length and the operating condition, which stands for the speed ( $V_{rev}$ ) were fixed during the optimization procedure.

The optimization problem can be mathematically expressed as represented by Eq. (7).

$$\text{minimize } f(X), (f: \Omega \subseteq \mathcal{R}^{n_x} \rightarrow \mathfrak{R}) \quad (7)$$

where  $n_x$  is the number of decision variables. It is highlighted that an optimization algorithm is focused on finding the optimal solution ( $X^*$ ) that minimizes  $f(X^*)$ ; i.e.,  $f(X^*) < f(X), \forall X \in \Omega$ , where  $\Omega$  denotes the search domain.

### 2.3 Surrogate-based optimization

A surrogate-based optimization procedure is an approach where direct optimization of the expensive high-fidelity simulation model is replaced by iterative updating and re-optimization of its computationally cheap representation; i.e., the surrogate. A SM is basically a mathematical model, which is considered a statistical response surface model of a simulation model [16-17].

There are several function approximation modelling techniques, where the SM is created by approximating sampled high-fidelity model data. The most commonly used methods to solve engineering problems include radial basis function interpolation, polynomial approximation, response surface methodology, weighted average surrogate, support vector regression, kriging, and neural networks [17-18].

SM provides a vector of prediction outputs ( $Y$ ) for a given vector of prediction inputs ( $X \in \mathcal{R}^{n_x}$ ), where  $n_x$  is the number of dimensions or the number of decision variables, and can be expressed as Eq. (8).

$$Y = f(X, X_t, Y_t) \quad (8)$$

where  $X_t \in \mathcal{R}^{n_x}$  and  $Y_t$  are the vectors of training inputs and outputs, respectively, which are used to build the SM *a priori*. In turn,  $X$  is the unknown point to be predicted by using the SM [17-18].

In the current work, Kriging-based genetic algorithm was used to approximate the functions based on various sample points. The SM is called low fidelity model, which is a reduced-accuracy but a fast representation of the system of interest. This can be obtained from several ways, such as by using simplified-physics, leaving out certain second-order effects or describing the system on a different physical level [16-19].

Kriging model could also be defined as an interpolating SM used to approximate the high fidelity computer models in a given design space. It is a linear combination of a known polynomial function,  $f(X)$ , and a local derivation,  $Z(X)$ , which follows a distribution with 0 mean and variance, expressed as  $\sigma^2$ . The model can be postulated as described in Eq. (9) [17-18].

$$Y(X) = f(X) + Z(X) \quad (9)$$

where  $Y(X)$  represents the unknown function of interest. The covariance matrix of  $Z(X)$  is given by Eq. (10).

$$\text{cov}[Z(X^{(i)}), Z(X^{(j)})] = \sigma^2 R[R(X^{(i)}, X^{(j)})]; i, j = 1 \dots n_x \quad (10)$$

where  $R$ ,  $n_x$  and  $R(X^{(i)}, X^{(j)})$  represent the symmetric correlation coefficient matrix of order  $(n_x, n_x)$  with normalized diagonal values, the number of samples and the spatial correlation function between the sample points  $X^{(i)}$  and  $X^{(j)}$ , respectively.

Two types of correlation functions can be used for the SM: the exponential (Ornstein-Uhlenbeck process) and the Gaussian correlation function, given by Eq. (11) and (12), respectively.

$$R(X^{(i)}, X^{(j)}) = \prod_{l=1}^{n_x} \exp(-\theta_l |X_l^{(i)} - X_l^{(j)}|) \quad (11)$$

$$R(X^{(i)}, X^{(j)}) = \prod_{l=1}^{n_x} \exp(-\theta_l (X_l^{(i)} - X_l^{(j)})^2) \quad (12)$$

where  $\theta_l \in \mathcal{R}^+$ . The number of hyperparameters ( $\theta$ ) is equal to the number of variables ( $n_x$ ).

To construct the Kriging model the software Matlab was used.

Figure 2 represents the optimization procedure used in this study. In general, the stages of surrogate-based modelling approach include an initial CFD study (defining of the geometry, the computational domain and the boundary conditions, and conducting a mesh dependency study before the achievement of the CFD results). The next stage consists of defining the objective functions and the variables involved in the optimization (goal setting). Subsequently, a sampling plan for the design points is defined; then, some numerical simulations at these design points are carried out for the construction of a new SM based on the simulations. Afterwards, by using a genetic algorithm, the optimal design points are found. If the optimal design points with the local maxima of the objective functions are not found in the design space, a new design space is generated, and the analysis is repeated in the new design space until the optimal design point with the local maximal is achieved [20].

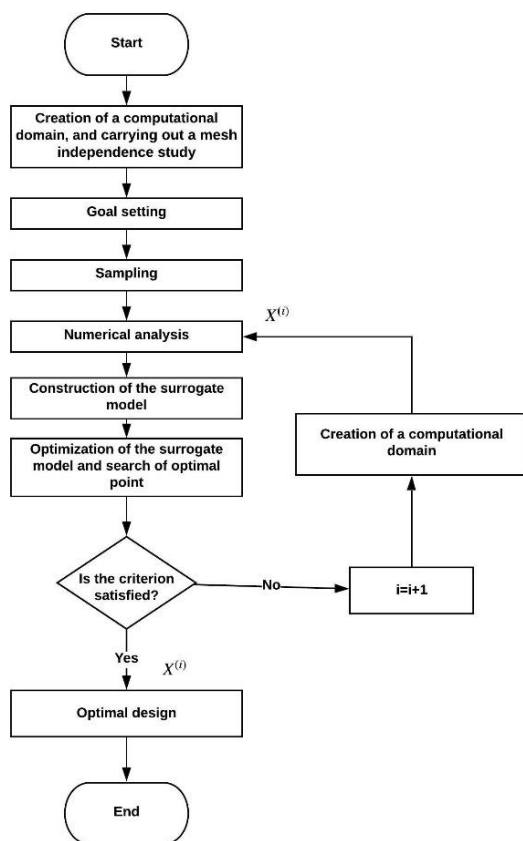


Fig. 2. Optimization procedure

When obtaining the optimal design points of the genetic algorithm, it is decided to evaluate in CFD the 3 points of the Pareto front with a better  $C_L$ ,  $C_D$ ,  $C_L/C_D$  ratio [4, 7]. Furthermore, for the point out of the three evaluated ones obtaining the best  $C_L/C_D$  ratio, additional studies are made by varying  $\alpha$  in the integer values close to the selected point up to a maximum  $C_L/C_D$  of the geometry is found. Once the results of the CFD simulations of the new design points are obtained, the data are added to the initial sampling to create a new mathematical model and an optimization cycle until the stop criterion is met [4, 8]. As a stop criterion, it was decided to evaluate the same number of new designs, including the initial sampling

plan, which corresponds to an evaluation of 100 multi-element hydrofoils for a total of 200 CFD simulations.

## 2.4 Optimal design search algorithm

Once the SM was constructed, a genetic algorithm was used to find the optimal design points [20]. For this propose, the function `gamultiobj` in Matlab was utilized, which was represented by Eq. (13). The function found  $X$  on the Pareto front of the objective functions defined by the variable “*fun*”. In turn, *nvars* was the dimension of the optimization problem (number of decision variables).

$$X = \text{gamultiobj}(\text{fun}, \text{nvars}) \quad (13)$$

## 2.5 Numerical analysis

For the optimization procedure, a traditional hydrofoil Eppler 420 was selected due to previous studies carried out by the authors where its performance was demonstrated in comparison with other hydrodynamic profiles [3-5]. A computational domain was designed in order to know the performance parameters of this hydrofoil as a multi-element hydrofoil. A two dimensional CFD model was used to describe the flow behaviour around the hydrofoil. The flow was assumed two-dimensional, steady, incompressible and viscous. The Reynolds-averaged Navier-Stoke (RANS) equations were considered as the governing equation with the  $k - \omega$  SST turbulence model. Numerical fluid flow simulations were performed using the commercial computer code Ansys Fluent. The  $C_{pre}$ ,  $C_L$  and the  $C_D$  were evaluated using the software.

A computational grid for an Eppler 420 multi-element hydrofoil is represented in Figure 3. The unstructured grids used in this study have a C-topology with quadrilateral elements. The computational domain stretches 10 chord lengths upstream (radius) and 20 chord lengths downstream. The mesh was built to ensure a  $y^+ \leq 1$  placing at least 30 layers in the region of the boundary layer. A study of the grid independence was conducted to ensure the solution convergence achieving a mesh of about 210000 elements.  $C_L$  and  $C_D$  were chosen as the parameters of interest for the mesh independence study. Grids for several design points were generated in a similar manner and the  $y^+$  value of the converged solution was maintained below 1. The boundary conditions are described in Table 12.

Table 2. Geometric hydrofoil and boundary condition specifications

Parameter	Description
Blade profile	Eppler 420
Blade chord length (C)	0.177 m
Fluid	Water at 25° C
Turbulence model	$k - \omega$ SST
Inlet	Velocity inlet
Outlet	Pressure outlet
Upper boundaries (top edge)	Symmetric boundary
Lower boundaries (bottom edge)	Symmetric boundary
Hydrofoil	No-slip wall

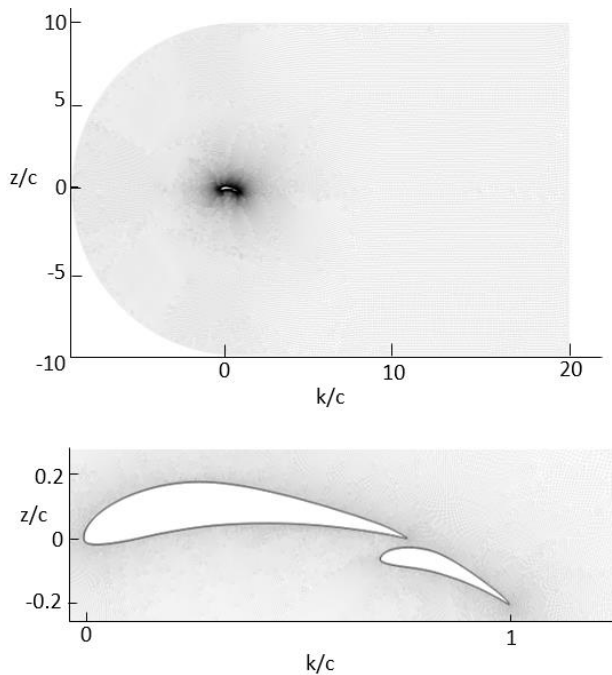


Fig. 3. a) A computational grid with a C-topology for an Eppler 420 multi-element hydrofoil. b) A view of the computational grid close to the Eppler 420 multi-element hydrofoil.

## 2 Results and discussion

For the construction of the SM based on the initial simulations, a process of generating data point was required. The performance of SM strongly depends on the quality, as well as on the number of samples. For this study 100 high-fidelity CFD initial simulations were carried out.

The initial points could be defined by a design of experiment (DoE) technique, which is an adaptive sampling strategy. On the other hand, stationary sampling strategies, such as Latin Hypercube Sampling (LHS), which are widely used, was utilized in the current research. LHS is a statistical method for generating a quasi-random sampling distribution [4]. Therefore, LHS was used with 100 points that were optimized according to the Morris-Mitchell criterion to ensure a uniform distribution of the sample points within the design space.

Subsequently, the design parameters, the objective functions and design space were defined. The geometry of the multi-element hydrofoil and the CFD analysis were conducted. The CFD solver evaluated the objective function values of the designs parameters. From these simulations, the SM was created using the data points analysed by the CFD solver. The search algorithm found the optimal point from the SM constructed.

Through the established SM, a Pareto front was constructed, as shown in Figure 4. In the figure, the results concerning the initial sampling, the design suggested by the SM, the starting design (Eppler 420 hydrofoil) and the selected multi-element design based on the  $C_L/C_D$  ratio are illustrated.

Figure 4 show that few of the initial designs contributed to the Pareto front and some of them granted a better  $C_L/C_D$  ratio than that corresponding to the starting Eppler 420 hydrofoil. Additionally, the designs supplied by the SM contributed to the Pareto front with new designs that fill the gaps in the Pareto front of the initial sampling plan and move it forward.

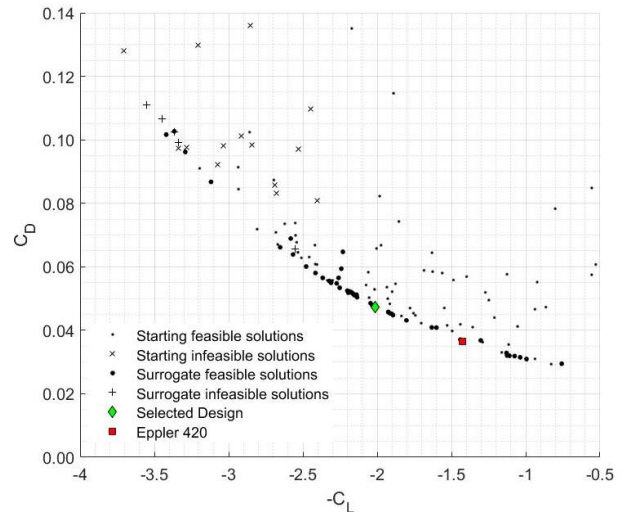


Fig. 4. Pareto front.

The initial and optimized multi-element hydrofoil shapes are represented in Figure 5. The resulting flow was more aligned with the flap compared to the traditional hydrofoil. The multi-element design selected as the optimal one had a gap of 2.825 % $C_1$ , an overlap of 8.52 % $C_1$ , a  $\delta$  of 19.765°, a  $C_2$  of 42.471 % $C_1$  and a  $\alpha$  of -4°.  $C_L$  and  $C_D$  were equal to 2.016 and 0.047, respectively, providing a  $C_L/C_D$  of 42.517. The variation of  $C_L$ ,  $C_D$  and  $C_L/C_D$  with  $\alpha$  are shown in Figure 6. It can be clearly observed that there was a large performance improvement of the optimized shape in comparison with the initial one (i.e.,  $C_L/C_D$  increased from 39.050 to 42.517).

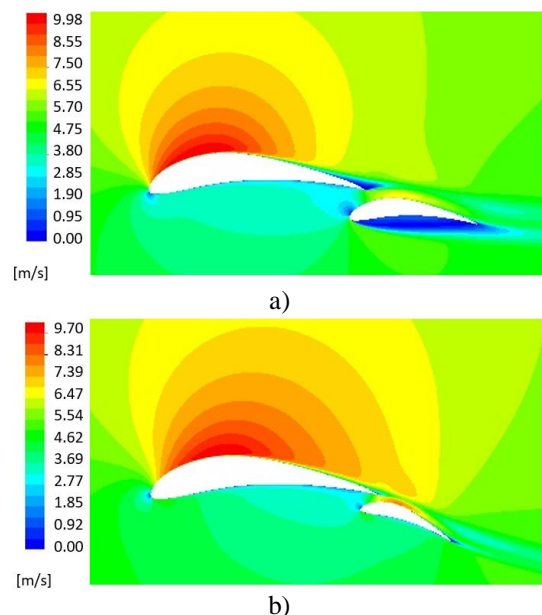


Fig. 5. Contours of velocity of the flow around the initial (a) and optimized (b) multi-element hydrofoil.

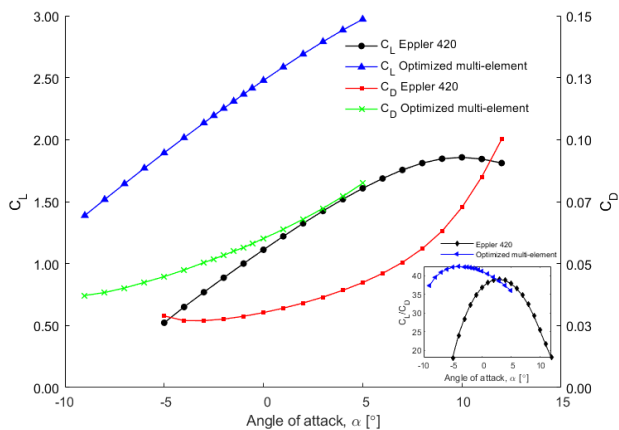


Fig. 6.  $C_L/C_D$  ratio as a function of  $\alpha$  for a traditional hydrofoil and for an optimized multi-element hydrofoil using the Eppler 420 profile.

#### 4. Conclusion

The design of a multi-element hydrofoil based on SM was presented in this study. The use of SM refers to an approach that can be employed for the design of hydrokinetic turbines, allowing the correction of a multi-element hydrofoil shape, aiming at preventing cavitation. In this study, the objective was to maximize  $C_L$  and minimize  $C_D$  subjected to  $C_{pre} < 4$  constraint. The results showed that the improvement of  $C_L/C_D$  is significant compared to the conventional hydrofoil. The multi-element hydrofoil had a  $C_L/C_D$  of 8.87 % larger than that of the traditional hydrofoil.

The design of the optimal hydrofoil for hydrokinetic appliances always requires an amount of time experiments and computational analysis in order to achieve the planned goals. In this work, the SM allowed reducing the time of multi-element hydrofoil design process involved in the blade manufacture of a horizontal axis hydrokinetic turbine due to the reduction iterations number and the CFD analysis within the optimization procedure.

#### Acknowledgement

The authors gratefully acknowledge the financial support provided by the Colombia Scientific Program within the framework of the call Ecosistema Científico (Contract No. FP44842- 218-2018).

#### References

[1] D. Kumar and S. Sarkar, "A review on the technology, performance, design optimization, reliability, techno-economics and environmental impacts of hydrokinetic energy conversion systems", *Renewable and Sustainable Energy Reviews*, (2016). Vol. 58, pp. 796-813.  
 [2] E. Chica and A. Rubio-Clemente, "Design of Zero Head Turbines for Power Generation", *Renewable Hydropower Technologies Basel I. Ismail*, IntechOpen, DOI: 10.5772/66907. Available from: <https://www.intechopen.com/books/renewable-hydropower-technologies/design-of-zero-head-turbines-for-power-generation>. July 26th 2017.  
 [3] E. Chica, J. Aguilar and A. Rubio-Clemente, "Analysis of a lift augmented hydrofoil for hydrokinetic turbines", *Renewable Energy and Power Quality Journal*, (2019). Vol. 17, pp. 49-55

[4] J. Aguilar, A. Rubio-Clemente, L. Velásquez and E. Chica, "Design and optimization of a multi-element hydrofoil for a horizontal-axis hydrokinetic turbine", *Energies*, (2019), Vol. 12 (4679), pp. 1-18.  
 [5] E. Chica, J. Aguilar and A. Rubio-Clemente, "Investigación numérica sobre el uso de álabes multi-elemento en turbina hidrocínética de eje horizontal", *Revista UIS Ingenierías*, (2019). Vol. 10 (3), pp. 117-128.  
 [6] E. Benini, R. Ponza and A. Massaro, "High-lift multi-element airfoil shape and setting optimization using multi-objective evolutionary algorithms", *Journal of Aircraft*, (2011). Vol. 48(2), pp. 683-696.  
 [7] P.M. Kumar, J. Seo, W. Seok, S.H. Rhee and A. Samad, "Multi-fidelity optimization of blade thickness parameters for a horizontal axis tidal stream turbine", *Renewable energy*, (2019). Vol. 135, pp. 277-287.  
 [8] A.I. Forrester, N.W. Bressloff and A.J. Keane, "Optimization using surrogate models and partially converged computational fluid dynamics simulations", *Proceedings of the Royal Society A: Mathematical, Physical and Engineering Sciences*, (2006). Vol 462(2071), pp. 2177-2204.  
 [9] R. Yondo, E. Andres and E. Valero, "A review on design of experiments and surrogate models in aircraft real-time and many-query aerodynamic analyses", *Progress in Aerospace Sciences*, (2018). Vol. 96, pp. 23-61.  
 [10] S. Jeong, M. Murayama and K. Yamamoto, "Efficient optimization design method using kriging model", *Journal of aircraft*, (2005). Vol. 42(2), pp. 413-420.  
 [11] J.D. Feldhacker, B.A. Jones, A. Doostan and J. Hampton, "Reduced cost mission design using surrogate models", *Advances in Space Research*, (2016). Vol. 57(2), pp. 588-603.  
 [12] V. Díaz-Casás, J.A. Becerra, F. Lopez-Peña and R.J. Duro, "Wind turbine design through evolutionary algorithms based on surrogate CFD methods", *Optimization and engineering*, (2013). Vol. 14(2), pp. 305-329.  
 [13] A.D.V. Carrasco, D.J. Valles-Rosales, L.C. Mendez and M.I. Rodriguez, "A site-specific design of a fixed-pitch fixed-speed wind turbine blade for energy optimization using surrogate models", *Renewable energy*, (2016). Vol. 88, pp. 112-119.  
 [14] A.F. Molland, A.S. Bahaj, J.R. Chaplin and W.M.J. Batten, "Measurements and predictions of forces, pressures and cavitation on 2-D sections suitable for marine current turbines", *Proceedings of the Institution of Mechanical Engineers, Part M: Journal of Engineering for the Maritime Environment*, (2004). Vol. 218(2), pp. 127-138.  
 [15] P.A.S.F da Silva, L.D. Shinomiya, T.F. de Oliveira, J.R.P. Vaz, A.L.A. Mesquita and A.C.P.B. Junior, "Design of hydrokinetic turbine blades considering cavitation", *Energy Procedia*, (2015). Vol. 75, pp. 277-282.  
 [16] N.V. Qoeipo, R.T. Haftka, W. Shyy, T. Goel, R. Vaidyanathan, and P.K. Tucker, "Surrogate-based analysis and optimization", *Progress in Aerospace Sci-ences*, (2005). Vol. 41 (1), pp. 1-28.  
 [17] A. Bhosekar and M. Ierapetritou, "Advances in surrogate based modeling, feasibility analysis, and optimization: A review", *Computers & Chemical Engineering*, (2018). Vol. 108, pp. 250-267.  
 [18] L. Leifsson, E. Hermansson and S. Koziel, "Optimal shape design of multi-element trawl-doors using local surrogate models", *Journal of Computational Science*, (2015). Vol. 10, pp. 55-62.  
 [19] Y. Jin, "A comprehensive survey of fitness approximation in evolutionary computation", *Soft computing*, (2005). Vol. 9(1), pp. 3-12.  
 [20] A.F.P. Ribeiro, A.M. Awruch and H.M. Gomes, "An airfoil optimization technique for wind turbines", *Applied Mathematical Modelling*, (2012). Vol. 36(10), pp. 4898-4907.